Journal of Fluorine Chemistry 131 (2010) 1039–1043

Contents lists available at ScienceDirect

Journal of Fluorine Chemistry

journal homepage: www.elsevier.com/locate/fluor

Local structural analyses on molten terbium fluoride in lithium fluoride and lithium–calcium fluoride mixtures

Masahiko Numakura [a,*], Yoshihiro Okamoto [b], Tsuyoshi Yaita [b], Hideaki Shiwaku [b], Hiroshi Akatsuka [a], Atsushi Nezu [a], Keisuke Tajima [a], Yasuaki Shimohara [a], Catherine Bessada [c], Olivier Pauvert [c], Didier Zanghi [c], Pierre Chamelot [d], Haruaki Matsuura [a,c,e]

[a] Research Laboratory for Nuclear Reactors, Tokyo Institute of Technology, 2-12-1-N1-10, Ookayama, Meguro-ku, Tokyo 152-8550, Japan
[b] Japan Atomic Energy Agency, Kansai Photon Science Institute, Kouto 1-1-1, Sayo-cho, Sayo-gun, Hyogo 679-5148, Japan
[c] Conditions Extrêmes et Matériaux: Haute Température et Irradiation, CNRS-UPR 3079, 1D Avenue de la Recherche Scientifique, 45071 Orléans Cedex 2, France
[d] Laboratoire de Génie Chimique, CNRS-UMR-5503, Université Paul Sabatier, 118 route de Narbonne, 31062 Toulouse Cedex 4, France
[e] le STUDIUM, 3D Avenue de la Recherche Scientifique, 45071 Orléans Cedex 2, France

ARTICLE INFO

Article history:
Received 28 April 2010
Received in revised form 21 July 2010
Accepted 26 July 2010
Available online 3 August 2010

Keywords:
X-ray absorption fine structure (XAFS)
Terbium fluoride
Lithium fluoride
Calcium fluoride
Molten salt

ABSTRACT

X-ray absorption fine structure (XAFS) measurements on terbium fluoride in molten lithium fluoride and in molten lithium–calcium fluoride mixtures, (e.g. 0.20TbF_3–0.80LiF, 0.20TbF_3–0.62LiF–0.18CaF_2, 0.20TbF_3–0.48LiF–0.32CaF_2, 0.50TbF_3–0.50LiF, and 0.50TbF_3–0.38LiF–0.12CaF_2), have been carried out. In the solid state, coordination number of terbium (N_i) and inter ionic distances between terbium and fluorine in the first neighbor (r_i) are nearly constant in all mixtures. In 0.20TbF_3–0.80LiF, 0.20TbF_3–0.62LiF–0.18CaF_2 and 0.50TbF_3–0.50LiF mixtures, N_i's decrease from ca. 8 to 6 and r_i's also decrease from ca. 2.29 to 2.26 Å on melting. On the other hands, in molten 0.20TbF_3–0.48LiF–0.32CaF_2 and 0.50TbF_3–0.38LiF–0.12CaF_2 mixtures, N_i's are slightly larger than 6 and r_i's do not change. These facts correspond to the amount of F^- supplied by solvent melts, i.e. the effect of CaF_2 becomes predominant at $b$$CaF_2 > 0.32$ in ternary 0.20TbF_3–aLiF–$b$$CaF_2$ mixtures and at $b$$CaF_2 > 0.12$ in ternary 0.50TbF_3–aLiF–$b$$CaF_2$ mixtures.

1. Introduction

Solid rare earth fluorides (LnF_x) are known for their important use in industrial applications (e.g. solid electrolyte [1] and optical materials [2]). In the molten state, the development of pyrochemical reprocessing of spent nuclear fuels in molten fluorides [3] or the molten salt nuclear reactor in nuclear engineering [4,5] requires a better knowledge of their structural and physico-chemical properties at high temperature. In a recent study, it has been reported that the LiF–CaF_2 eutectic melt can be used as solvent for the electrodeposition of Nd and Th, while LiF–NaF and LiF–KF eutectic melts cannot be used for the same purpose theoretically [6]. However, the structure of LnF_x and actinide fluorides (AnF_x) in LiF–CaF_2 eutectic melt has not been clarified yet. To clarify the correlation between structure and physico-chemical properties would be useful to find the better electrolysis condition in order to develop the pyrochemical reprocessing.

Knowledge on the structural information of some molten fluorides and their mixture melts has been obtained by using Raman, nuclear magnetic resonance (NMR) and X-ray absorption fine structure (XAFS) spectroscopies. It is observed that in $x$$LnF_3$–$(1-x)$KF molten mixtures Ln^{3+} cations predominantly take octahedral configuration at $x_{LnF_3} < 0.25$ by Raman spectroscopy [7,8]. By XAFS experiments, coordination numbers of Ln^{3+} in pure molten LnF_3 have been determined as between 6 and 7. For heavier lanthanide fluoride melts, 6-coordination becomes predominant. The coordination number of Ln^{3+} in molten $x$$LnF_3$–$(1-x)$MF (Ln = La–Nd, Sm–Gd, Dy–Er, Yb, Lu and Y, M = Li, Na, K) ($x_{LnF_3} = 0.2$) binary systems have been shown slightly lower values than those in pure molten LnF_3 [9,10]. On the other hands, the coordination number around Y^{3+} in YF_3–LiF mixtures is not considered to be 6 but more likely 7 or 8 by NMR spectroscopy [11]. So the structure of molten LnF_3 and its mixtures still has to be clarified systematically. Especially, the structure of molten ternary LnF_3–LiF–CaF_2 systems has not been reported yet, thus the correlation between structure and physico-chemical properties has to be examined.

In this study, 0.20TbF_3–0.80LiF (20Tb–80Li), 0.20TbF_3–0.62LiF–0.18CaF_2 (20Tb–62Li–18Ca), 0.20TbF_3–0.48LiF–0.32CaF_2 (20Tb–48Li–32Ca), 0.50TbF_3–0.50LiF (50Tb–50Li), and 0.50TbF_3–0.38LiF–0.12CaF_2 (50Tb–38Li–12Ca) mixtures are specially focused for the structural investigation. The variation of the local structure around Tb^{3+} by an addition of CaF_2 is discussed in this paper.

* Corresponding author. Tel.: +81 3 5734 3379; fax: +81 3 5734 3379.
E-mail address: numakura.m.aa@m.titech.ac.jp (M. Numakura).

0022-1139/$ – see front matter © 2010 Elsevier B.V. All rights reserved.
doi:10.1016/j.jfluchem.2010.07.011

2. Results and discussion

The XAFS oscillations of terbium, $k^3\chi(k)$, and the corresponding radial structural functions, $FT|k^3\chi(k)|$, obtained in 20Tb–80Li mixture at various equilibrated temperatures are shown in Fig. 1(a) and (b), respectively. The structural parameters obtained by the curve fitting analysis are listed in Table 1. Initial structural model for the curve fitting of EXAFS spectra in solid state was taken from the literatures [12,13], i.e. Tb^{3+} is surrounded by $4F^-$ at 2.25 Å and $4F^-$ at 2.32 Å and the average value is ca. 2.29 Å. The main phase of 20Tb–80Li was confirmed to be $LiTbF_4$ by powder X-ray diffraction [14], thus the curve fitting result of solid state is consistent with $LiTbF_4$. As shown in Fig. 1(a) and (b), the decrease of XAFS oscillation in $k^3\chi(k)$ with increasing temperature reflects an increase of thermal fluctuations. Especially, in $k^3\chi(k)$, drastic decrease of XAFS oscillation was observed between 873 and 1023 K and the 1st peak intensity in $FT|k^3\chi(k)|$ also decreased considerably. It has been confirmed that the melting point of this sample was 956 K by differential scanning calorimetry [14], which perfectly corresponded to the value reported in the phase diagram [15]. Thus, these spectral variations clearly correspond to the melting of the sample. As shown in Table 1, N_i's decreased from 8 to 6 and r_i's also decreased from ca. 2.29 to 2.26 Å by melting. The Debye–Waller factors gradually increased with increasing of thermal fluctuation. This tendency of the variation of N_i's on melting is consistent with the other $x\mathrm{LnF_3}$–$(1-x)$LiF ($x_{\mathrm{LnF_3}} = 0.20$) systems and the value of r_i in molten phase is located between those in $0.20GdF_3$–0.80LiF and $0.20DyF_3$–0.80LiF [9]. These facts suggest that r_i of the first Ln^{3+}-F^- correlation mainly depends on the size of Ln^{3+}.

The curve fitting results as well as the experimental data on molten 20Tb–62Li–18Ca, 20Tb–48Li–32Ca, 50Tb–50LiF, and 50Tb–38Li–12Ca mixtures are shown in Fig. 2(a) and (b). The structural parameters of solid and molten states are also shown in Table 1. N_i's and r_i's in all solid states were almost constant. This fact indicates that the first neighbor shell around Tb^{3+} is similar to the others in solid states. Quite similar values of N_i's and r_i's in molten binary 20Tb–80Li and 50Tb–50Li mixtures were obtained by curve fitting analysis. However, it is conjectured that the structures of 20Tb–80Li and 50Tb–50Li mixtures should be slightly different. In

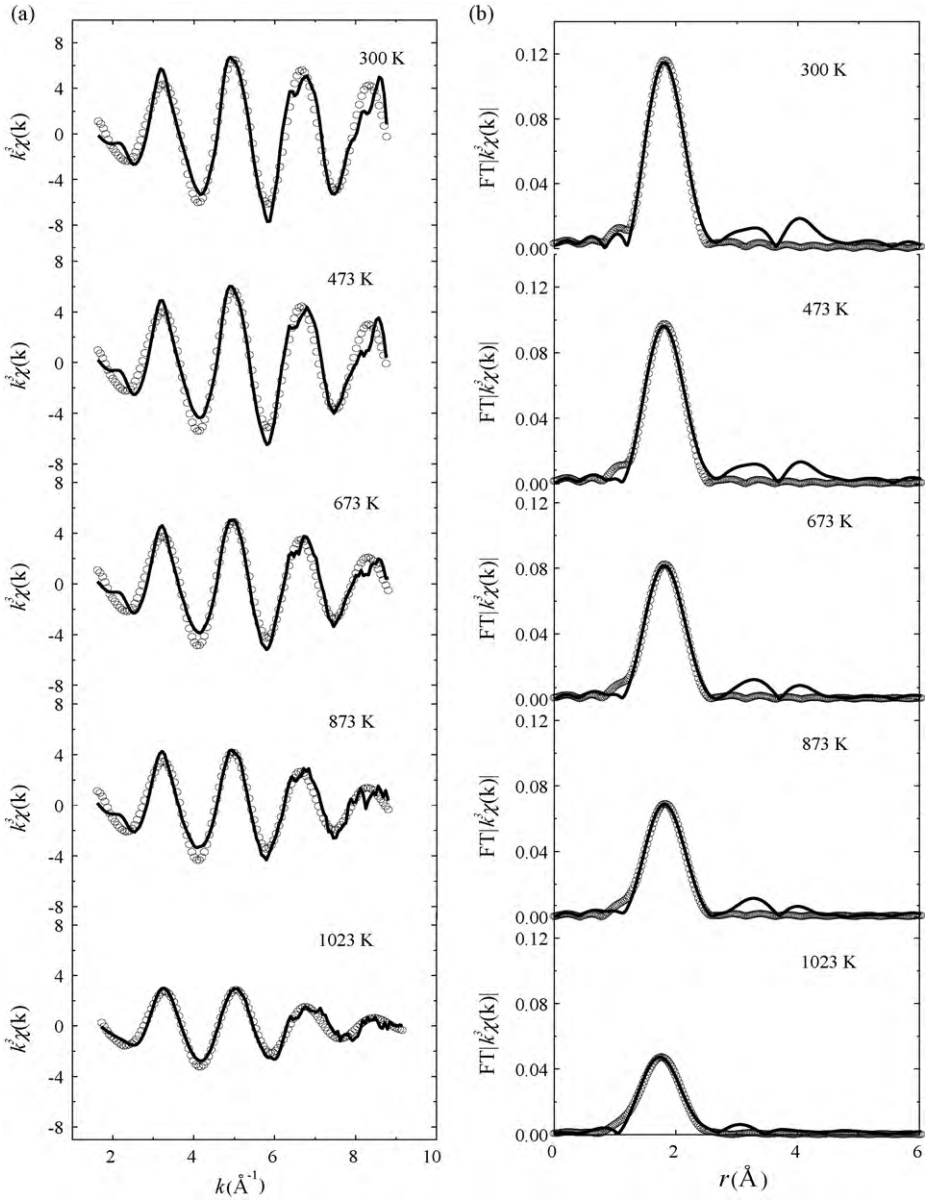

Fig. 1. (a) and (b) Tb L_{III}-edge XAFS oscillations, $k^3\chi(k)$, and radial structural functions, $FT|k^3\chi(k)|$, of 20Tb–80Li at various equilibrated temperatures.

Table 1
Structural parameters of solid and molten TbF_3–LiF and TbF_3–(LiF–CaF_2) systems.

Samples F^-/Tb^{3+}	T (K)	N_i*	r_i (Å)**	σ^2 (10^{-2} Å^2)	C_3 (10^{-3} Å^3)	C^4 (10^{-4} Å^4)	R***
0.20TbF_3–0.8LiF (20Tb–80Li) (Tb^{3+}:F^- = 1:7)	300	7.9_7	2.28_9	0.55 ± 0.01	0 (fix)	0 (fix)	5.44
	473	8.0 ± 0.1	2.29_1	0.82 ± 0.07	0 (fix)	0 (fix)	6.40
	673	7.9 ± 0.1	2.29_3	1.03 ± 0.03	0 (fix)	0 (fix)	4.45
	873	8.1 ± 0.3	2.29_5	1.40 ± 0.01	0 (fix)	0 (fix)	3.55
	1023	6.0 ± 0.2	2.26 ± 0.01	1.71 ± 0.02	0.16 ± 0.06	0.75 ± 0.20	5.49
0.20TbF_3–0.62LiF–0.18CaF_2 (20Tb–62Li–18Ca) (Tb^{3+}:F^- = 1:7.92)	300	8.2 ± 0.1	2.28_9	0.67 ± 0.02	0 (fix)	0 (fix)	4.99
	573	8.2 ± 0.1	2.28_3	1.07 ± 0.02	0 (fix)	0 (fix)	8.96
	873	8.1_9	2.28_8	1.49 ± 0.01	0 (fix)	0 (fix)	7.99
	1073	5.8 ± 0.3	2.26 ± 0.01	1.99 ± 0.02	0.17 ± 0.11	3.30 ± 1.31	7.31
0.20TbF_3–0.48LiF–0.32CaF_2 (20Tb–48Li–32Ca) (Tb^{3+}:F^- = 1:8.6)	300	8.3 ± 0.3	2.28_9	0.69 ± 0.04	0 (fix)	0 (fix)	6.28
	573	7.9 ± 0.2	2.28_9	0.96 ± 0.05	0 (fix)	0 (fix)	7.43
	873	8.2 ± 0.4	2.29_2	1.56 ± 0.04	0 (fix)	0 (fix)	7.30
	1073	6.8 ± 0.4	2.30 ± 0.01	2.46 ± 0.25	0.18 ± 0.15	2.04±1.68	8.54
0.50TbF_3–0.50LiF (50Tb–50Li) (Tb^{3+}:F^- = 1:4)	300	8.1_1	2.29_5	0.58 ± 0.02	0 (fix)	0 (fix)	7.95
	1173	5.9 ± 0.1	2.25_9	1.96 ± 0.10	0.44 ± 0.24	1.02 ± 0.66	7.88
0.50TbF_3–0.38LiF–0.12CaF_2 (50Tb–38Li–12Ca) (Tb^{3+}:F^- = 1:4.23)	300	8.1_2	2.29_6	0.64 ± 0.02	0 (fix)	0 (fix)	4.54
	573	8.3 ± 0.2	2.29_9	0.98 ± 0.02	0 (fix)	0 (fix)	4.45
	873	8.0 ± 0.2	2.29_1	1.44 ± 0.08	0 (fix) 0	(fix)	6.11
	1073	6.7 ± 0.4	2.30 ± 0.01	2.90 ± 0.12	0.08 ± 0.07	0.49 ± 0.23	8.46

*, **The significant figures were evaluated to be 2 and 3 for the coordination number and the bond distance considering the potential error of XAFS, although the statistical errors were less than 0.1 and 0.01 by curve fitting respectively. ***Residual is defined as $R = \sum_{i=1}^{N} |k^3\chi_{exp}(k) - k^3\chi_{cal}(k)| / \sum_{i=1}^{N} |k^3\chi_{exp}(k)|$

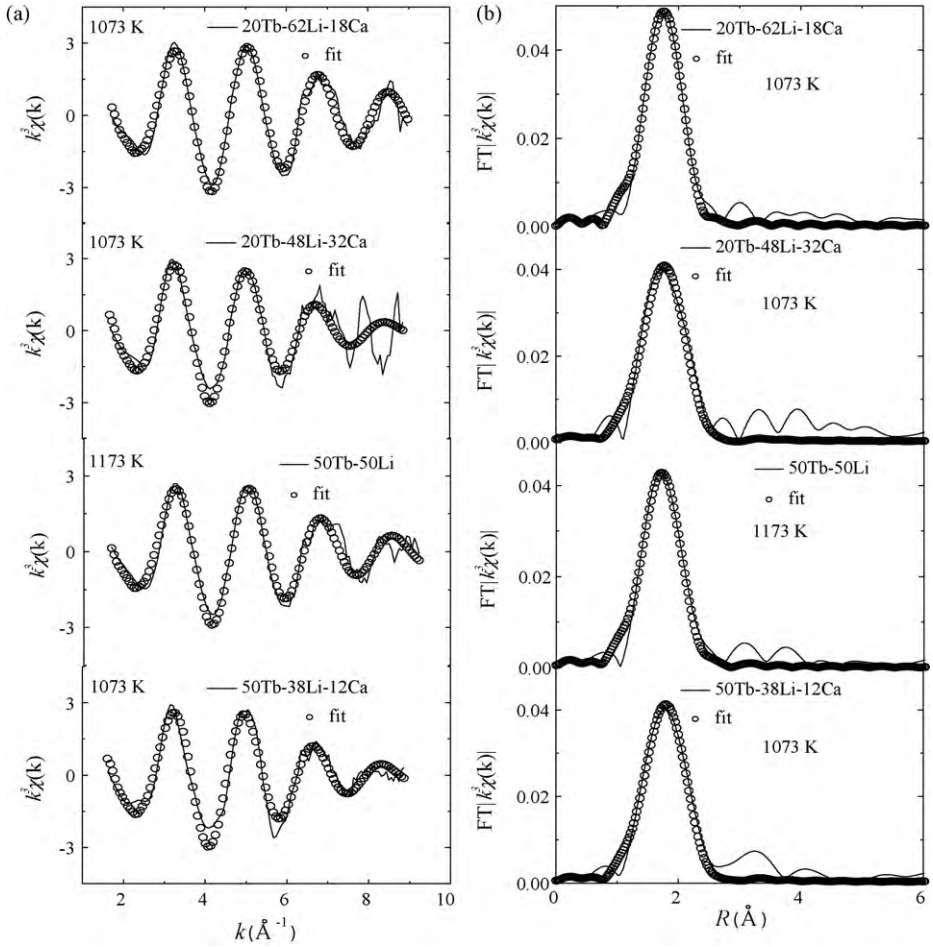

Fig. 2. (a) and (b) Tb L_{III}-edge XAFS oscillations, $k^3\chi(k)$, and radial structural functions, FT$|k^3\chi(k)|$, of molten 20Tb–62Li–18Ca, 20Tb–48Li–32Ca, 50Tb–50Li, 50Tb–38Li–12Ca.

20Tb–80Li mixture, more than 6 times amount of F^- can exist around Tb^{3+}, thus the isolated octahedral configuration, $(TbF_6)^{3-}$, can be formed. On the contrary, only 4 times amount of F^- can exist around Tb^{3+} in 50Tb–50Li mixture, thus the octahedral configurations should be connected to the other octahedral configurations to compensate the number of F^-, i.e. the octahedral configurations are connected by the edge or corner sharing. The edge sharing means that octahedral configurations connect via two F^- with neighbor octahedral configurations, and the corner sharing means that octahedral configurations connect via one F^- with neighbors. Similar structural configurations have been suggested by Raman spectroscopy, molecular dynamics and XAFS in other halide systems [7,8,16–18], e.g. in molten xYBr$_3$–$(1-x)$LiBr system, destruction of the networking structure is promoted in the xYBr$_3 < 0.5$ [19]. It is considered that the difference among these structures affects physico-chemical properties, since diffusion coefficient, conductivity, viscosity and mixing enthalpy depend on the structural change in various systems [20–22].

In molten 20Tb–62Li–18Ca mixture, N_i and r_i were quite similar to those in 20Tb–80Li mixture, thus the similar octahedral configuration was formed. On the other hand, in ternary 50Tb–38Li–12Ca and 20Tb–48Li–32Ca mixtures, N_i's decreased from 8 to 6.7 and 6.8 and r_i's did not change on melting. (These errors may be slightly larger than the other systems.) In addition, the Debye–Waller factors were relatively larger than those of the rest of the mixtures investigated. Therefore, the local structure around Tb^{3+} tends to vary by an addition of CaF_2 depending on concentration. It is conjectured that the difference among structural variation in molten phase relates to the amount of F^- supplied by solvent melts. In 20Tb–48Li–32Ca mixture, the largest amount of F^- is supplied by the solvent melts among all mixtures investigated, i.e. Tb^{3+}: F^- = 1.8.6. Thus N_i would indicate slightly larger than 6. In ternary 0.50TbF$_3$–aLiF–bCaF$_2$ mixtures, the effect of CaF_2 would appear more strongly. Some part of networking structure would be broken by addition of even small amount of CaF_2 (bCaF$_2$ = 0.12). Since N_i's increase from 6 to 6.7 or 6.8 in 50Tb–38Li–12Ca and 20Tb–48Li–32Ca mixtures, the local structure around Tb^{3+} tends to be asymmetric and then the Debye–Waller factor would be larger than those of the rest of the mixtures investigated.

The slightly different tendency has been observed in binary 0.20LnF$_3$–0.80MF (Ln = La–Nd, Sm–Gd, Dy–Er, Yb, Lu and Y, M = Li, Na, K) by EXAFS analysis [9], i.e. the local structure around Ln^{3+} in mixture system at xLnF$_3$ = 0.20 does not depend on the species of alkali metal fluorides. However, N_i tends to increase by addition of CaF_2. It is conjectured that alkaline earth fluoride would have different solvent effect from alkali fluoride. In a recent study, it has been reported that the structural disorder around La^{3+} in molten chlorides by the mixing with divalent cation, e.g. Mg^{2+}, is much larger than by the mixing with alkali cations and these facts are related to the ionic radii of cations, number densities of Cl^- and charges of solvent melts [23]. There would be a common feature both in fluoride and chloride systems, thus the solvent effect in molten fluoride systems should be investigated in detail using other techniques.

3. Experimental

XAFS measurements in transmission mode were performed at BL27B beamline at Photon Factory, KEK, Tsukuba, Japan. Tb L_{III}-edge (7.519 keV) XAFS spectra were collected with a fixed time scan method by using Si (1 1 1) double crystal monochromator. Mixtures of TbF_3 (Aldrich. 5N), LiF (Soekawa Co. 4N) and CaF_2 (Soekawa Co. 4N) except 50Tb–50Li were melted in a glassy carbon crucible at ca. 1073 K in a glove box filled with an argon atmosphere in high purity. (In the case of 50Tb–50Li, the mixture was melted at ca. 1173 K.) Then, they were mixed with boron nitride powder (BN, Showa Denko Co. ltd), and pressed into pellets in 0.7–1.0 mm diameter and 1 mm thickness. The mixing weight ratio of TbF_3 to BN was ca. 1:4–4.5. It has been found that if the source of oxidation (e.g. moisture) as impurity exists in an electric furnace, TbF_3 reacts with BN to be $TbBO_3$ at ca. 1073 K [14]. Therefore, to prevent chemical reaction during heating process in XAFS measurements, these pellets were installed in a cell made with boron nitride [24,25] and the electric furnace was filled with He gas at ca. 30 kPa.

Temperatures of the samples in XAFS measurements were derived by the calibration curve, which had been obtained by the difference between the values of two thermocouples located at the sample and the sample holder for a temperature controller. We have decided the temperature of XAFS measurement from the phase diagram of binary xTbF$_3$–aLiF [15]. The melting point of xTbF$_3$–aLiF–bCaF$_2$ has not been reported yet. However these samples have been molten definitely below 1073 K, since they were melted once in a glassy carbon crucible at 1073 K at the sample preparation. EXAFS data were analysed by using the WinXAS ver.3.1 [26]. Fitting parameters were derived by using the equation as follows.

$$\chi(k) = \sum_i S_i \frac{N_i F_i(k)}{k r_i^2} \exp\left(-2k^2\sigma_i^2 + \frac{2}{3}C_4 k^4\right) \times \sin\left(2kr_i + \phi_i(k) - \frac{4}{3}C_3 k^3\right)$$

where S_i is probability of single electron excitation, N_i: coordination number of F^- around Tb^{3+}, r_i: distance from Tb^{3+} to F^-. σ: Debye–Waller factor that indicates thermal and structural disorder, C_3 and C_4: third and fourth cumulants, these indicate anharmonic vibration effect at high temperature, $F_i(k)$ and $\phi_i(k)$: backscattering amplitude and phase shift of photoelectron, respectively. In the curve fitting, we adopted the cumulant expansion (3rd and 4th cumulant) method [27] to obtain the more reliable structural parameters of TbF_3 mixture melts. On the other hand, both cumulants were fixed to be 0 until 873 K, since an anharmonic vibration effect could be ignored in these systems. $F_i(k)$ and $\phi_i(k)$ were calculated from the FEFF 8.00 code [28]. Curve fitting analysis was performed several times both in k-space, $k^3\chi(k)$, and r-space, FT$|k^3\chi(k)|$, to obtain structural parameters and these structural parameters and errors in Table 1 were obtained statistically. The temperature dependence in the molten state is relatively smaller than in solid state in EXAFS spectra, thus the structural parameters in molten states shown in Table 1 do not reflect any important temperature dependence.

4. Concluding remarks

The local structure of 20Tb–80Li, 20Tb–62Li–18Ca, 20Tb–48Li–32Ca, 50Tb–50Li, and 50Tb–38Li–12Ca mixtures at various temperatures were investigated by XAFS. In 20Tb–80Li, 50Tb–50Li and 20Tb–62Li–18Ca mixtures, N_i's decreased from 8 to 6 and r_i's also decreased from ca. 2.29 to 2.26 Å by melting. In 20Tb–48Li–32Ca and 50Tb–38Li–12Ca mixtures, N_i's were slightly larger than 6 and r_i's did not change. These facts would relate to the amount of F^- supplied by solvent melts. The local structure around Tb^{3+} tends to vary by addition of CaF_2 and this variation appears at bCaF$_2 > 0.32$ in ternary 0.20TbF$_3$–aLiF–bCaF$_2$ mixtures and at bCaF$_2 > 0.12$ in ternary 0.50TbF$_3$–aLiF–bCaF$_2$ mixtures by XAFS. In 20Tb–62Li–18Ca and 50Tb–38Li–12Ca mixtures, the local structure around Tb^{3+} tends to be asymmetric and structural disorder would be larger than those of the rest of mixtures investigated. In

order to draw more practical structural images, other experimental techniques and MD simulation should be performed.

Acknowledgements

This work was financially supported by the PACEN CNRS programs (PCR-ANSF and PARIS). This study was done by the research cooperation agreements between Japan Atomic Energy Agency and Tokyo Institute of Technology as well as the CEMHTI, CNRS and RLNR, Tokyo Institute of Technology. XAFS experiments have been carried out with the approvals of the Photon Factory Program Advisory (Proposal Nos. 2008G065, 2009G093, 2009G544).

References

[1] S. Yonezawa, S. Nishibu, M. Leblanc, M. Takashima, J. Fluor. Chem. 128 (2007) 438–447.
[2] H. Takahashi, S. Yonezawa, M. Kawai, M. Takashima, J. Fluor. Chem. 129 (2008) 1114–1118.
[3] R. Takagi, H. Matsuura, Y. Fujii-e, R. Fujita, M. Kawashima, Prog. Nucl. Energy 29 (1995) 471–476.
[4] S.K. Oh, K.M. Chung, Nucl. Eng. Des. 216 (2002) 11–19.
[5] J. Vergnes, D. Lecarpentier, Nucl. Eng. Des. 207 (2001) 43–67.
[6] P. Chamelot, L. Massot, C. Hamel, C. Nourry, P. Taxil, J. Nucl. Mater. 360 (2007) 64–74.
[7] V. Dracopoulos, B. Gillbert, B. Borrensen, G.M. Photiadis, G.N. Papatheodorou, J. Chem. Soc. Faraday Trans. 93 (1997) 3081–3088.
[8] V. Dracopoulos, B. Gillbert, G.N. Papatheodorou, J. Chem. Soc. Faraday Trans. 94 (17) (1998) 2601–2604.
[9] S. Watanabe, Doctor Thesis, Tokyo Institute of Technology, 2006.
[10] H. Matsuura, S. Watanabe, H. Akatsuka, Y. Okamoto, A.K. Adya, J. Fluor. Chem. 130 (2009) 53–60.
[11] C. Bessada, A. Rakhmatullin, A.-L. Rollet, D. Zanghi, J. Fluor. Chem. 130 (2009) 45–52.
[12] R.E. Thoma, G.D. Brunton, R.A. Penneman, T.K. Keenan, Inorg. Chem. 9 (1970) 1096–1101.
[13] C. Keller, H. Schmutz, J. Inorg. Nucl. Chem. 27 (1965), S. 900-01.
[14] M. Numakura, C. Bessada, S. Ory, A. Rakhmatullin, H. Akatsuka, A. Nezu, T. Yaita, Y. Okamoto, H. Shiwaku, H. Matsuura, The 41st Symposium on Molten Salt Chemistry, 2009, pp. 97–98 (in Japanese).
[15] R.E. Thoma, Progress in Science and Technology of the Rare Earth, vol. 2, Pergamon Press, New York, 1966, p. 110.
[16] G.N. Papatheodorou, J. Chem. Phys. 66 (1977) 2893–2900.
[17] W.J. Glover, P.A. Madden, J. Chem. Phys. 121 (2004) 7293–7303.
[18] R. Takagi, F. Hutchinson, P.A. Madden, A.K. Adya, M. Gaune-Escard, J. Phys. Condens. Matter 11 (1999) 645–658.
[19] Y. Okamoto, M. Akabori, H. Motohashi, H. Shiwaku, T. Ogawa, J. Synchrotron Radiat. 8 (2001) 1191–1199.
[20] M. Salanne, C. Simon, P. Turq, P.A. Madden, J. Phys. Chem. B 111 (2007) 4678–4684.
[21] Y. Okamoto, T. Ogawa, Z. Naturforsch, Teil. A 54 (1999) 91–94.
[22] Y. Okamoto, T. Ogawa, Z. Naturforsch, Teil. A 54 (1999) 544–604.
[23] Y. Okamoto, S. Suzuki, H. Shiwaku, A. Ikeda-Ohno, T. Yaita, P.A. Madden, J. Phys. Chem. A 114 (13) (2010) 4664–4671.
[24] A.-L. Rollet, C. Bessada, Y. Auger, P. Melin, M. Gailhanou, D. Thiaudiere, Nucl. Instrum. Methods B 226 (2004) 447–452.
[25] C. Bessada, A.-L. Rollet, D. Zanghi, O. Pauvert, C. Thefany, H. Matsuura, B. Sitaud, P.L. Solari, "A double barrier cell for high temperature EXAFS experiments in molten actinides fluoride mixtures" Actinide-XAS-2008, 5th Workshop on Speciation, Techniques, and Facilities for Radioactive Materials at Synchrotron Light Sources, Workshop Proceedings, Saint-Aubin, France, 15–17 July 2008. Publication of the OECD/Nuclear Energy Agency, 2009, pp. 117–122.
[26] T. Ressler, J. Synchrotron Radiat. 5 (1998) 118–122.
[27] G. Bunker, Nucl. Instrum. Methods Phys. Res 207 (1983) 437–444.
[28] A.L. Ankudinov, B. Ravel, J.J. Rehr, S.D. Conradson, Phys. Rev. B 58 (1998) 7565–7567.